A COMPARATIVE STUDY OF HILLSLOPE AND SLOPE SEGMENT APPROACHES IN A SEMI-DISTRIBUTED INFLOW PREDICTION MODEL

Thattanaporn KHOMSRI [1*], ***Chatchai TANTASIRIN*** [1], ***Venus TUANKRUA*** [1].

DOI: 10.21163/ GT_2026.211.02

ABSTRACT

Accurate inflow prediction models are essential decision-support tools for effective reservoir management and optimal water resource utilization. Among semi-distributed hydrological models, the hillslope-based approach has traditionally offered the finest spatial resolution. However, this study explores the integration of a higher-resolution spatial discretization method—slope segments—originally introduced by Tantasirin et al. (2016) for soil erosion modeling, into inflow prediction modeling for reservoir systems in the Lam Phra Phloeng watershed, Thailand. The Lam Phra Phloeng watershed was subdivided into 4,839 hillslope units and 54,378 slope segments. Compared to hillslopes, slope segments provided more homogeneous spatial units, reducing internal variability in land use and soil properties. This refinement allowed for more representative Curve Number (CN) values, enhancing the accuracy of runoff estimation using the SCS-CN method. Model performance was evaluated using three metrics—Percentage Error in Peak Flow (PEPF), Root Mean Square Error (RMSE), and Nash–Sutcliffe Efficiency (NSE)—during the validation years 2015, 2019, and 2020. The slope segment-based model consistently outperformed the hillslope-based model. For example, PEPF values were significantly lower (0.18%, 0.18%, and 2.02% vs. 1.25%, 1.47%, and 7.01%), RMSE values were reduced (0.61, 1.23, and 4.32 MCM vs. 0.66, 1.50, and 4.48 MCM), and NSE values were higher (0.94, 0.36, and 0.44 vs. 0.90, 0.30, and 0.40). These results demonstrate that slope segment-based spatial subdivision enhances the predictive performance of inflow models and offers a promising approach for improving hydrological modeling in reservoir systems. Future applications in diverse watersheds could further validate its utility for water resource planning and management.

Key-words: *SCS-CN model; Spatial discretization; Slope segment delineation; Reservoir inflow prediction*

1. INTRODUCTION

Reservoirs are typically formed by constructing dams across streams, with their primary function being the regulation of natural streamflow. This regulation is achieved by storing excess water during wet seasons and releasing it during dry periods to mitigate low river flows. Accurate inflow forecasting is particularly critical during the rainy season, as it directly informs reservoir drainage planning and operational decision-making. A wide range of inflow prediction models are employed as decision-support tools in reservoir management. These models are generally classified based on their spatial representation into three categories: lumped, semi-distributed, and distributed models.

Semi-distributed hydrological models rely on spatial discretization schemes to represent heterogeneity in land use, soils, and topography. Different schemes have been proposed, including sub-catchments, hydrological response units (HRUs), representative elementary areas (REA), geomorphological units, and hillslopes. Each has advantages and weaknesses: sub-catchments reduce computational time but may obscure variability; HRUs capture heterogeneity but are often not spatially explicit; REAs aim for optimal process homogeneity at a given scale; while hillslopes provide finer spatial representation but can still encompass diverse soils and land uses.

---

[1]*Faculty of Forest, Department of Conservation, Kasetsart University, Thailand. *Corresponding author (TK) janjao.geo@gmail.com; (CT) fforcct@ku.ac.th; (VT) ffor.venus@gmail.com.*

The scale of these units directly influences runoff timing, volume predictions, and water balance estimates (Beven, 1993; Reggani et al., 1998; Vannametee et al., 2012, 2013).

While finer units can preserve spatial heterogeneity, they also increase the number of modeling elements, raising challenges of parameterization and computation. Semi-distributed models therefore aim to identify an optimal spatial scale that balances realism with efficiency. Hillslopes are widely used but may remain too coarse for representing local hydrological processes. In response, Tantasirin et al. (2016) introduced slope segments, which subdivide hillslopes into smaller, hydrologically connected planes delineated by stream links and contour lines. These units are more homogeneous in soil and land use properties, and are directly connected to local drainage networks.

Based on this background, we hypothesize that slope segment discretization will improve inflow prediction compared to traditional hillslope units. Specifically, slope segments reduce aggregation errors in land use–soil combinations, yield more representative Curve Number (CN) values, and better capture flow connectivity along hillslopes. At the same time, the scale remains compatible with semi-distributed modeling frameworks, avoiding the parameter burden of fully distributed models. This study evaluates the performance of slope segments against hillslopes to test this hypothesis.

In Thailand, the most commonly used lumped model is the Artificial Neural Network (ANN) model (Suiadee &Tingsanchali,2007; Chiamsathit,2016; Ngamsanroaj et al.,2019; Amnatsan,2021). Distributed models such as the HO8 (Kompor,2021) and wflow_sbm (Wannasin et al.,2021) have also been applied, while the Soil and Water Assessment Tool (SWAT) (Phomcha et al.,2021) serves as a representative semi-distributed model.

Lumped models treat each sub-basin as a single, homogeneous unit. While this approach simplifies computation and enables faster forecasts, it also generalizes spatial variability—such as rainfall-runoff dynamics—across the entire sub-basin. This can lead to parameter inaccuracies and reduced predictive performance. In contrast, distributed models incorporate detailed spatial data, including soil properties, vegetation, and land use, and divide the basin into fine-resolution grids. These models simulate water flow across cells, enabling runoff estimation at ungauged locations and assessments of water quality and land-use impacts (Smith et al.,2004) However, their high computational demands and long processing times can be limiting factors (Ejaz et al.,2022).

Semi-distributed models offer a compromise between these two approaches. They provide a more realistic representation of spatial heterogeneity than lumped models while requiring less computational power than fully distributed models (Tantasirin et al.,2016). These models typically use spatial units such as hydrological response units (HRUs), irregular grids, or hillslopes. Among these, hillslope-based models represent the finest level of spatial subdivision currently used in many semi-distributed frameworks (Flugel,1995). Hillslopes are key hydrological units that channel water to river networks via surface and subsurface pathways (Lapides et al.,2022), and are often divided into three zones: left, right, and top slopes (Fan et al.,2019).

Despite their finer resolution, hillslopes can still encompass large and heterogeneous areas. The size of these computational units significantly influences hydrological responses (Zehe et al.,2014). Larger units may obscure spatial variability, leading to less accurate parameterization and reduced model fidelity (Hutchinson, 1988; Kienzle, 2003; Jha, 2004; Rouhani, 2009). To address this, Tantasirin et al. (2016) introduced a method for subdividing hillslopes into smaller, more homogeneous units called slope segments, initially for soil erosion modeling. However, this finer-scale spatial discretization has not yet been adopted in semi-distributed inflow prediction models.

This study aims to incorporate slope segment-based spatial subdivision into inflow prediction modeling for reservoirs and to evaluate its performance relative to traditional hillslope-based models. By comparing the predictive accuracy of these two approaches, the study seeks to determine whether slope segment discretization can enhance model performance. Improved inflow forecasting has the potential to significantly strengthen reservoir water resource management, particularly in the face of increasing challenges posed by land-use changes and climate variability. Ultimately, more accurate modeling will support more efficient and equitable water allocation across the watershed.

2. MATERIALS AND METHODS

2.1. Automated drainage network extraction

The automated drainage network extraction method proposed by Tantasirin et al. (2016) was adopted, integrating spatial hydrological analysis with Digital Elevation Model (DEM) processing. A 10-m resolution DEM was generated using the ANUDEM algorithm (Hutchinson, 1988; Hutchinson, 1989), followed by hydrological preprocessing to correct topographic depressions ("sinks") using the efficient sink-filling method of Wang & Liu (2006). Flow direction and accumulation were computed using the Rho8 algorithm (Fairfield & Leymarie, 1991), and the Lam Phra Phloeng Dam outlet was designated as the watershed outlet. The Drainage Area Threshold (DAT), which determines stream initiation points, was defined to balance hydrological detail with computational efficiency.

Hydrological and spatial datasets used in this study were compiled from official government agencies (**Table 1**). Rainfall data were obtained from the Thai Meteorological Department (TMD) and the Royal Irrigation Department (RID), while streamflow and reservoir inflow records were provided by RID. Contour maps were sourced from the Royal Thai Survey Department (RTSD) and subsequently converted into a DEM, while land use/cover and soil datasets were supplied by the Land Development Department (LDD). These datasets form the basis for model input, calibration, and validation.

Table 1.

Summary of datasets used in this study.

Dataset	Variable(s)	Source	Units	Resolution	Period
Rainfall gauges	Daily (mm)	TMD & RID	Station points	Daily	2010–2023
Streamflow	Q (m^3/s)	RID	Station points	Daily	2010–2023
Inflow	MCM	RID	Station points	Daily	2010–2023
Contour	Elevation (m)	RTSD	Shapefile	-	2023
DEM	Elevation (m)	Generated from contour data	Raster	10*10 m	2023
Land use/cover	LULC classes	LDD	Shapefile	-	2011,2015,2019
Soil	HSG / texture	LDD	Shapefile	-	2023

2.2. Determination of the Optimal Drainage Area Threshold (DAT)

To identify the optimal DAT, the Number of Error Stream Cells (NESC) method was applied by Tantasirin et al. (2016). Stream networks were extracted using DAT values ranging from 10,000 to 500,000 m^2. The optimal threshold was determined using the Power Rule derivative, identifying the point where error reduction plateaued. The selected DAT of 450,000 m^2 (4,453 cells) minimized spatial errors and was used for subsequent watershed segmentation.

2.3. Slope Segment-Based Spatial Delineation

Following stream extraction, the watershed was subdivided into hydrological units using a hillslope-based approach (Lapides et al., 2022) dividing each sub-watershed into left, right, and upper hillslopes. These hillslopes were further refined into slope segments using Tantasirin's method.

Stream links were extended and segmented at 100-meter intervals, with adjacent land areas defined as slope planes. These were then subdivided along contour lines to form slope segments—smaller, more homogeneous units that enhance spatial resolution. The delineation was implemented using a custom-developed script (**Fig. 1**). To achieve finer spatial resolution, each hillslope unit was further subdivided using the slope segment method introduced by Tantasirin. This method begins by extending the stream links within each hillslope unit. These extended stream links are then segmented at 100-meter intervals, producing a series of stream segments. The land area adjacent to each stream segment is defined as a slope plane. Each slope plane is subsequently subdivided based on contour lines derived from elevation data, resulting in smaller and more homogeneous spatial units known as slope segments (**Fig. 2**). This hierarchical delineation process enhances the spatial granularity of the model, allowing for more accurate representation of hydrological processes. The final delineation of slope segments was implemented using a custom-developed script.

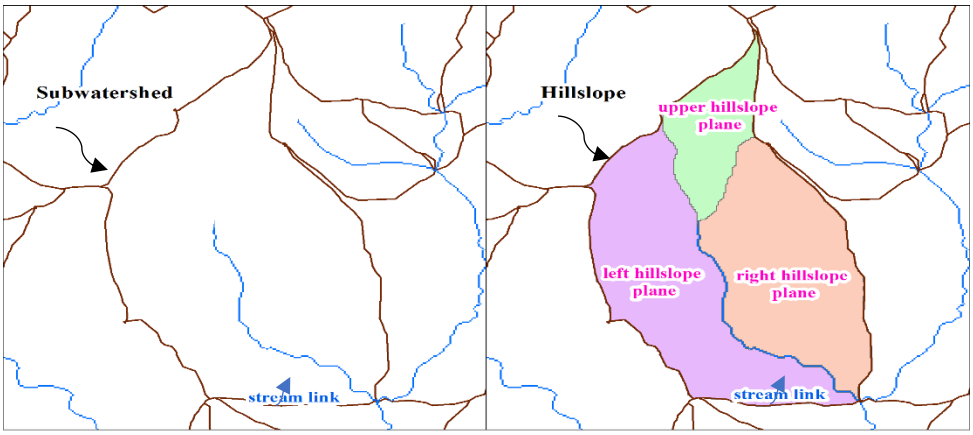

Fig. 1. Sub-watershed delineation and corresponding hillslope units within the Lam Phra Phloeng watershed, illustrating the spatial hierarchy used in the semi-distributed hydrological model.

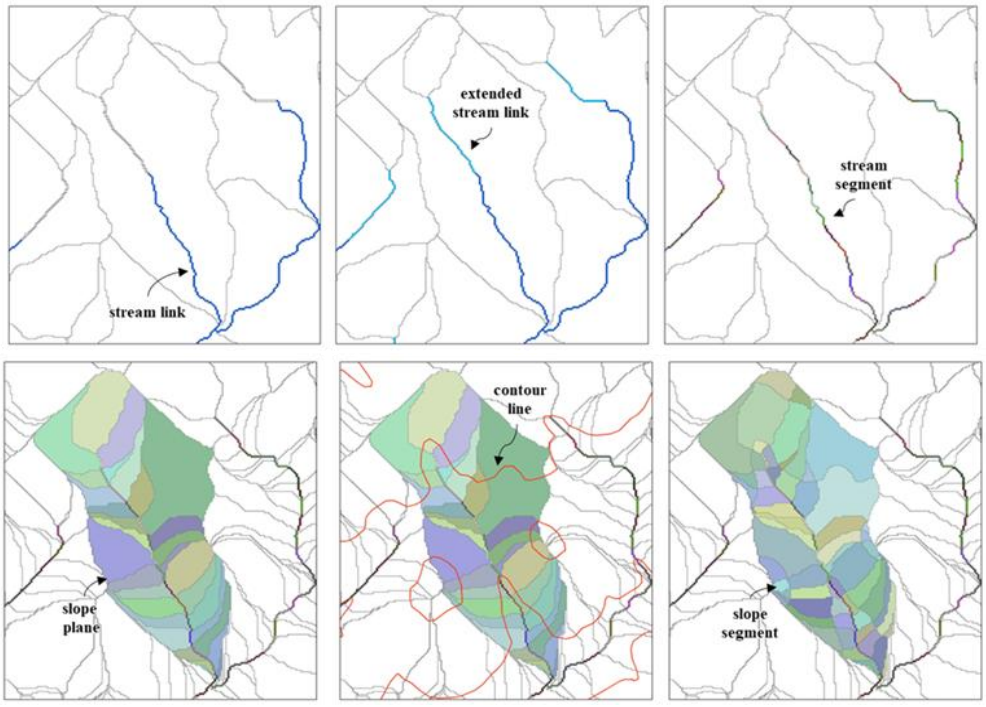

Fig. 2. Procedure for refining hillslope boundaries to smaller, more hydrologically representative units, adapted from Tantasirin, aimed at improving spatial resolution and runoff response accuracy in watershed modeling.

2.4. Reservoir Inflow Modeling

2.4.1. SCS–Curve Number Implementation and Inflow Modeling

The SCS–Curve Number (SCS–CN) method was applied to estimate surface runoff into the Lam Phra Phloeng Reservoir, Thailand. This empirical method is widely used in data-scarce regions due to its simplicity and minimal input requirements (Soil Conservation Service, 1986). It has also been successfully applied in hillslope runoff estimation and spatial runoff modeling in Europe (Crăciun et al., 2007; Crăciun et al., 2009; Haidu & Ivan, 2016; Haidu et al., 2017) and Asia (Tripathi et al., 2006; Lian et al., 2020; Ngamsanroaj & Tamee, 2019).

2.4.2. CN Assignment and Antecedent Moisture Adjustment

Curve Number (CN) values were assigned to each spatial unit based on hydrologic soil group (HSG), land use (LU), and antecedent moisture condition (AMC). AMC adjustment followed USDA (2004) guidelines, using 5-day cumulative rainfall thresholds: CN I: < 35 mm and CN III: > 75 mm

This dynamic adjustment allows the model to account for soil wetness between storm events, improving runoff estimation accuracy (Crăciun et al., 2007). The distribution of HSG–LU combinations across hillslope and slope segment units is summarized in **Table 3** and **Fig. 6**, showing that slope segments preserve greater spatial heterogeneity than hillslopes.

2.4.3. Runoff Calculation

Daily runoff depth for each unit was computed using a custom Python script, implementing the standard SCS–CN equation:

$$Q = \frac{(P-0.2S)^2}{P+0.8S} 3^{f_0 rP} > 0.2S \quad (1)$$

$$S = \frac{254000}{CN} - 245 \quad (2)$$

where: Q = direct runoff (mm); P = total rainfall (mm); S = potential maximum retention after runoff begins (mm); CN = curve number adjusted for AMC.

2.4.4. Routing to the Reservoir

Runoff depth (mm) was converted to volume by multiplying by the unit area (m²). Volumes from all units were routed downstream via the *D8 flow direction network* derived from the DEM. Daily inflow to the reservoir pour point was obtained by summing contributions from all upstream units. Channel hydraulics were not explicitly simulated, consistent with a semi-distributed modeling approach.

2.4.5. Performance Metrics

Model performance was evaluated using three metrics:

$$RMSE = \sqrt{\left(\frac{1}{n}\sum_{t=1}^{n}(Q_t^{sim} - Q_t^{obs}\right)^2} \quad (3)$$

$$NSE = 1 - \frac{\sum_{t=1}^{n}(Q_t^{sim} - Q_t^{obs})^2}{\sum_{t=1}^{n}(Q_t^{obs} - \bar{Q_t}^{obs})^2} \quad (4)$$

$$PEPF = 100 * \frac{\left(Q_{peak}^{\{sim\}} - Q_{peak}^{\{obs\}}\right)}{Q_{peak}^{\{obs\}}} \quad (5)$$

where: Q^{Sim} and Q^{Obs} are simulated and observed reservoir inflows at time t; $\bar{Q}^{\text{Obs}}$ is the mean observed inflow.

These metrics allow evaluation of both overall hydrograph similarity (RMSE, NSE) and peak flow prediction accuracy (PEPF) (**Fig. 9**).

2.5. Rainfall-Runoff Data Preparation

Hydrological data from 2012–2023 were used, including daily runoff from Stations M.145 and M.171, and inflow data for the Lam Phra Phloeng Reservoir, all sourced from the Royal Irrigation Department (RID). Rainfall data from 10-gauge stations were evaluated for consistency using the Double Mass Curve (DMC) method (Searcy & Hardison,1960), with R^2 used to assess reliability. To account for climate variability, years were categorized by ENSO phase: La Niña: 2013, 2020; Neutral: 2012, 2015, 2018, 2021–2023; El Niño: 2014, 2016, 2017, 2019 Average rainfall was estimated using the Thiessen Polygon method (Arianti et al.,2018) (**Fig. 3**).

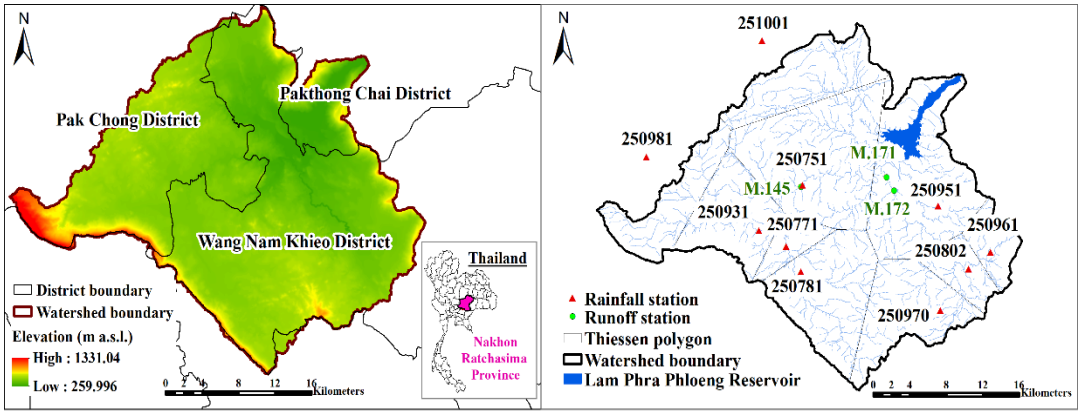

(a) (b)

Fig. 3. Study area and DEM (a); Rainfall and Runoff station in The Lam Phra Phloeng watershed (b).

2.6. Determination of Curve Number (CN)

CN values were derived from HSG and land use data provided by the Land Development Department of Thailand. HSGs were classified following Thephasit and Kriangsiri (Thephasit & Kriengsiri, 2001) into: Group A (high infiltration capacity): Soil Groups 29, 31, 38, 44, 47, 56 Group B (moderately high infiltration capacity): Soil Groups 33, 48, 55, 62 and Group D (low infiltration capacity): Water bodies. These classifications are illustrated in **Fig. 4**.

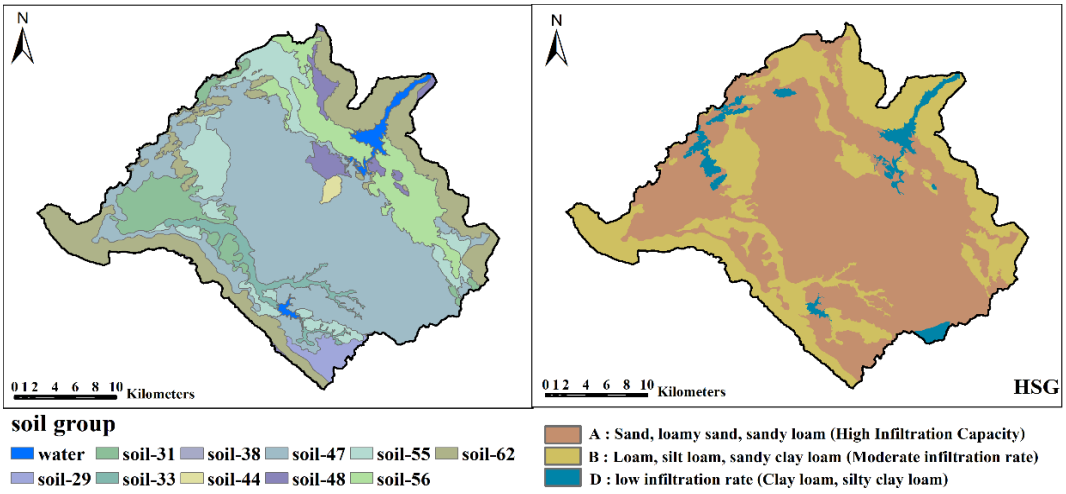

(a) (b)

Fig. 4. Classification derived from 15 soil groups in the Lam Phra Phloeng watershed (a); categorized into Groups A, B, and D based on infiltration capacity (b).

Land use was reclassified into nine categories (e.g., evergreen forest (For_evg), deciduous forest (For_dec), forest plantation (For_plant), rehabilitation forest (For_rehab): includes degraded forests, grasslands, shrublands, and wetlands , paddy fields (A_pad), field crops (A_crp), perennial plantations (A_tree), urban areas (Urb) and water bodies (Wat) and matched to rainfall-runoff years (e.g., 2011 land use for 2012–2013). To ensure temporal consistency with rainfall-runoff datasets, land use data (**Fig. 5**) were matched to the corresponding years: 2011 land use for 2012–2013 (La Niña and Neutral years); 2015 land use for 2014–2015 (El Niño and La Niña years); 2019 land use for 2018–2019 (Neutral and El Niño years). Spatial layers (hillslopes/slope segments, rainfall, HSG, land use) were integrated using raster union and zonal statistics to assign dominant attributes. CN values were then assigned using USDA (2004) (**Table 2** and **Fig. 6**).

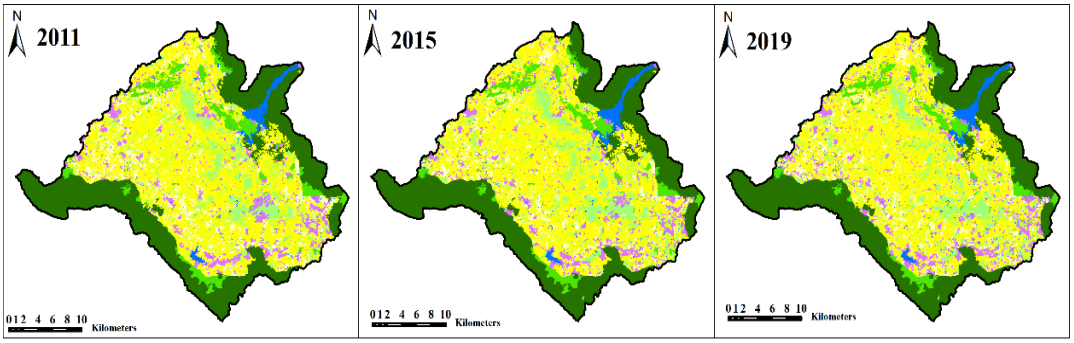

(a) (b) (c)

Fig. 5. Reclassified land use categories in the Lam Phra Phloeng watershed, grouped into nine hydrologically relevant classes for Curve Number assignment: 2011 (a); 2015 (b); 2019 (c).

Table 2.

Initial CN values.

Land Use	HSG		
	A	B	D
For_evg	33.08	57.75	60.00
For_dec	36.75	63.00	76.65
For_plant	42.00	69.30	78.75
For_rehab	47.25	73.50	80.85
A_pad	63.00	84.00	87.15
A_crp	74.09	85.00	89.00
A_tree	52.50	78.75	84.00
Urb	89.25	89.25	89.25
Wat	100.00	100.00	100.00

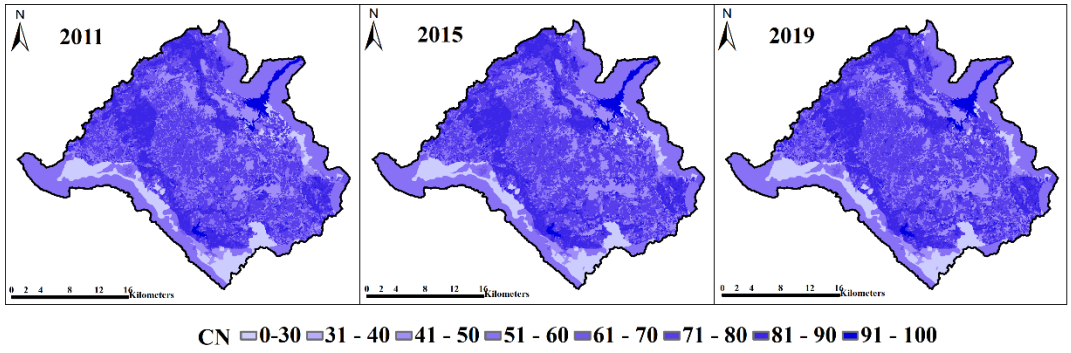

(a) (b) (c)

Fig. 6. Initial Curve Number (CN) values assigned to each spatial unit based on the intersection of land use and Hydrologic Soil Group (HSG) data, following USDA standard guidelines: 2011 (a), 2015 (b), 2019 (c).

2.7. Model calibration and validation

Given the sensitivity of the SCS-CN method to land use and Hydrologic Soil Group (HSG), a detailed analysis of Curve Number (CN) distribution was conducted for the calibration and validation years. Across the 2011, 2015, and 2019 land use datasets, the dominant types were field crops (A_crp), evergreen forest (For_evg), and rehabilitation forest (For_rehab), with A_crp showing a notable increase over time. The most extensive CN–HSG combinations were: AA_crp: 43.33% (hillslopes), 36.83% (slope segments) and BFor_evg, BA_crp, and AFor_evg followed in area coverage.

Sensitivity analysis revealed that AA_crp had the greatest influence on runoff predictions, significantly affecting PEPF, NSE, and RMSE. Calibration used data from 2012–2014 (La Niña, Neutral, El Niño), while validation applied 2015, 2019, and 2020 datasets. CN values for AA_crp were fine-tuned using a trial-and-error approach in the developed scripts. Model performance was assessed using: PEPF: Peak flow error (%), with values near zero indicating accuracy (Zhang et al., 2013; Kocyigit et al., 2017; Wang et al., 2025); RMSE: Measures average prediction error; values <50% of the observed standard deviation are acceptable (Sing et al., 2004); NSE: Indicates model efficiency (Nash & Sutcliffe, 1970; Waseem al., 2017).

3. RESULTS AND DISCUSSION

3.1. Watershed Subdivision into Hillslopes and Slope Segments

3.1.1. Number of Spatial Units

The Lam Phra Phloeng watershed was initially subdivided into 4,839 hillslope units and 54,378 slope segment units (**Fig. 7**). To improve computational efficiency and ensure timely forecasting, spatial units smaller than 0.1 km² (for hillslopes) and 0.03 km² (for slope segments) were excluded. This resulted in 1,738 hillslope units, covering 97.0% of the watershed area, and a slope segment model retaining 96.9% of the area. Model testing confirmed that excluding the smallest 3% of the area had no significant impact on performance metrics (PEPF, RMSE, NSE), while reducing simulation time by approximately 15 minutes per cycle.

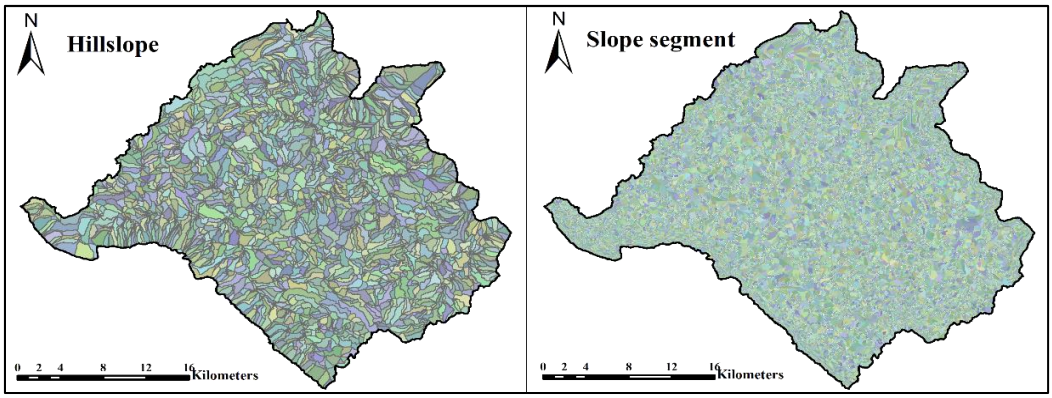

(a) (b)

Fig. 7. Spatial delineation of the Lam Phra Phloeng watershed into hydrological modeling units: Hillslope units (a), Slope segment units (b).

3.1.2. Hydrologic Soil Group (HSG) and Land Use (LU) Distribution

As shown in **Table 3**, the distribution of HSGs remained relatively stable across the original, hillslope, and slope segment models. Group A soils dominated, accounting for over 63% in all cases. However, land use distributions varied significantly. For example, in 2011: A_crp (field crops) increased from 39.26% in the original data to 51.32% in the hillslope model and 45.65% in the slope segment model. For rehab (rehabilitation forest) decreased from 10.23% to 4.55% (hillslope) and 6.74% (slope segment). Urban areas (Urb) and water bodies (Wat) also showed reduced representation in both models. This pattern was consistent across 2015 and 2019, with A_crp consistently increasing in both models, especially in the hillslope-based approach. These changes reflect how spatial aggregation can influence land use representation; a phenomenon also observed in other studies. For instance, in the Makiogawa River Basin (Japan), varying cell sizes led to different estimates of dominant land cover (Fong & Kawata, 2019). Similarly, Gebrie and Ludwig found that subbasin resolution affected land use proportions in the Blue Nile Basin Gebre & Ludwig, 2014).

Table 3.

Land use (LU) and Hydrologic Soil Group (HSG–LU) distributions calculated by zonal statistics.

Year	Dataset	For_evg	For_rehab	A_crp	A_tree	Urb	Wat	Other	Sum (%)
2011	Original	27.02	10.23	39.26	9.61	6.03	2.01	5.84	100
	Hillslope	29.11	4.55	51.32	4.65	3.86	1.1	5.41	100
	Slope seg	26.41	6.74	45.65	8.29	5.27	1.79	5.85	100
2015	Original	26.86	11.3	40.87	7.03	6.14	2.25	5.55	100
	Hillslope	28.63	5.95	53.18	2.6	3.35	1.19	5.1	100
	Slope seg	26.24	8.18	47.16	5.76	5.16	1.94	5.56	100
2019	Original	26.49	11.17	40.01	8.03	6.8	2.33	5.17	100
	Hillslope	28.45	5.77	52.82	3.04	4.09	1.16	4.67	100
	Slope seg	25.14	5.85	46.39	6.57	0.51	1.79	13.75	100

Percentages in each scenario (Original, Hillslope, Slope segment) sum ≈100%. Small differences (<±0.5%) are due to dominant-class assignment within units and area thresholds.

3.1.3. HSG–LU Combinations and Spatial Heterogeneity

The integration of HSG and LU data revealed further differences between the two models. As shown in **Table 4** and **Fig. 8**, the most dominant combination was AA_crp (Group A soil + field crops), which increased from 30.94% in the original data to 41.04% in the hillslope model and 36.34% in the slope segment model for 2011. Similar trends were observed in 2015 and 2019.

Table 4.

Distribution (%) of combined Hydrologic Soil Group and Land Use (HSG–LU) classifications.

Group	2011			2015			2019		
	orig	hlslp	slpseg	orig	hlslp	slpseg	orig	hlslp	slpseg
AFor_evg	7.80	7.73	7.71	7.67	7.32	7.58	7.43	7.16	7.37
AFor_dec	0.00	0.00	0.00	0.02	0.00	0.01	0.02	0.00	0.00
AFor_plant	3.45	3.54	3.49	3.28	3.24	3.38	3.00	3.01	3.17
AFor_rehab	8.59	4.34	5.96	9.49	5.37	7.10	9.28	5.04	7.00
AA_pad	0.27	0.02	0.21	0.20	0.07	0.16	0.20	0.06	0.17
AA_crp	30.94	41.04	36.34	32.09	43.03	37.39	31.53	42.91	36.77
AA_tree	7.35	3.80	6.32	5.38	2.11	4.41	6.16	2.36	5.10
AUrb	4.49	2.88	3.96	4.54	2.30	3.75	5.00	2.77	4.14
BFor_evg	18.56	20.71	18.06	18.53	20.67	18.04	18.43	20.68	17.86
BFor_dec	0.05	0.00	0.06	0.05	0.00	0.06	0.05	0.00	0.01
BFor_plant	1.53	1.36	1.53	1.46	1.24	1.42	1.43	1.22	1.37
BFor_rehab	1.44	0.17	0.64	1.49	0.25	0.78	1.55	0.35	0.87
BA_pad	0.22	0.10	0.24	0.22	0.15	0.22	0.19	0.08	0.18
BA_crp	7.81	9.66	8.83	8.24	9.69	9.28	7.93	9.51	9.12
BA_tree	2.03	0.83	1.78	1.50	0.50	1.23	1.71	0.68	1.36
BUrb	1.21	0.60	1.00	1.33	0.83	1.12	1.54	1.11	1.38
DFor_evg	0.65	0.66	0.64	0.65	0.65	0.63	0.63	0.61	0.60
DFor_dec	0.00	0.00	0.00	0.00	0.00	0.00	0.00	0.00	0.05
DFor_plant	0.31	0.40	0.33	0.30	0.40	0.31	0.30	0.30	0.30
DFor_rehab	0.19	0.04	0.15	0.32	0.33	0.30	0.33	0.39	0.34
DA_pad	0.00	0.00	0.00	0.00	0.00	0.00	0.00	0.00	0.00
DA_crp	0.51	0.62	0.48	0.55	0.46	0.49	0.56	0.40	0.51
DA_tree	0.23	0.01	0.19	0.15	0.00	0.12	0.17	0.00	0.11
DUrb	0.33	0.39	0.31	0.27	0.21	0.29	0.26	0.21	0.28

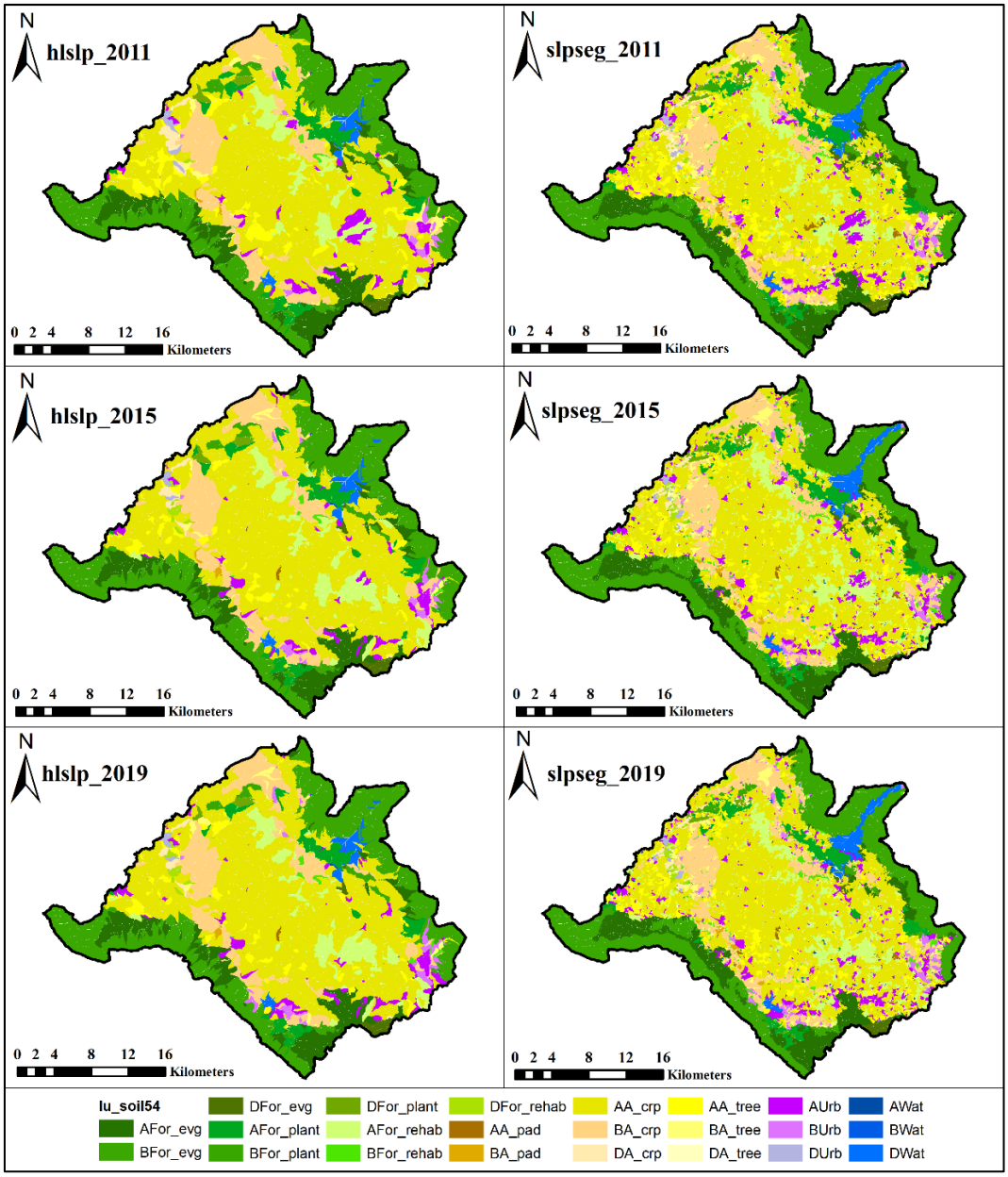

(a) (b)

Fig. 8. Distribution of Hydrologic Soil Groups (HSG) and Land Use (LU) types across different spatial discretizationsHillslope units (hlslp) (a); Slope segment units (slpeg) (b).

Other combinations, such as BFor_evg and BA_crp, also showed variation between models. The slope segment model generally preserved more heterogeneity due to its finer spatial resolution. For example, in a large hillslope unit containing multiple HSGs and LU types, area-weighted averaging was used to assign a single representative classification. In contrast, slope segments—being smaller—often retained distinct classifications, such as BA_crp instead of AA_crp, which can lead to higher predicted runoff due to higher CN values. This example illustrates how discretizing hillslopes into slope segments enhances spatial heterogeneity, improving the model's ability to represent variations in land use and soil properties, which are critical for accurate runoff prediction.

3.2. Comparison of Inflow Prediction Accuracy

3.2.1. Influence of CN Values on Runoff Prediction

Across all six years of simulation, both the hillslope and slope segment methods demonstrated that increasing the Curve Number (CN) led to higher total runoff volumes. This is expected, as higher CN values indicate reduced rainfall retention capacity, resulting in more surface runoff. The optimal CNII value for the AA_crp (Group A soil + field crops) combination was determined to be 81.5, compared to the USDA (2004) handbook value of 74.9. This 10% increase aligns with findings from Wang et al. (2025) and Lian et al. (2020), who also reported that CN values often need to be adjusted upward from USDA recommendations to improve model accuracy. Lian et al. found CN values up to 33% higher than USDA tables. Using slope segments improves land use–HSG homogeneity, which reduces CN averaging errors. This leads to more realistic initial abstraction and effective rainfall, and better peak timing through routing along locally connected planes.

3.2.2. Model Accuracy: Calibration and Validation

To complement the annual hydrograph comparisons, we conducted an event-based evaluation across the validation years. Rainfall–runoff events were extracted using a threshold of daily rainfall ≥10 mm, and corresponding peak inflows were identified. For each event, Percentage Error in Peak Flow (PEPF), Root Mean Square Error (RMSE), and Nash–Sutcliffe Efficiency (NSE) were computed for both hillslope and slope segment models. **Table 5** summarizes the average and variability (mean ± SD) of event-based metrics. Across all events, the slope segment model consistently achieved lower PEPF, smaller RMSE, and higher NSE than the hillslope model. Model performance was evaluated using PEPF, RMSE, and NSE metrics. The slope segment method consistently outperformed the hillslope method during both calibration and validation phases (**Table 5, Fig. 9**). However, in 2020, both models showed unsatisfactory accuracy. This was attributed to a mismatch in rainfall distribution: while 2013 (calibration year) experienced widespread rainfall, 2020 (validation year) saw heavy rainfall only in the upper and middle watershed. This spatial inconsistency led to inaccurate peak flow predictions. As shown in **Table 5**, heterogeneity preservation was enhanced, which links directly to improved performance metrics such as PEPF and NSE. Event-based evaluation across all validation years (2012–2015, 2019–2020) is summarized in the table. Slope segment units consistently outperform hillslope units, with higher PEPF and NSE and lower RMSE, particularly in years with heterogeneous land use–soil distributions. This suggests that finer representation of local connectivity and CN assignment improves peak discharge timing and overall simulation accuracy (Moriasi et al., 2007; Vannametee et al., 2013).

Table 5.

Event-based performance comparison of hillslope and slope segment units across calibration and validation years.

Period	Unit type	Number of events	PEPF (%)	RMSE (m^3/s)	NSE
Calibration	Hillslope	3	3.93 ± 3.03	2.97 ± 1.06	0.68 ± 0.05
	Slope segment	3	0.34 ± 1.04	2.71 ± 1.16	0.79 ± 0.03
Validation	Hillslope	3	3.91 ± 3.21	2.21 ± 2.00	0.53 ± 0.31
	Slope segment	3	0.79 ± 0.99	2.05 ± 1.56	0.59 ± 0.31

Values are mean ± standard deviation (SD) across multiple rainfall–runoff events. PEPF: peak error in peak flow (%), RMSE: root mean square error (m^3/s), NSE: Nash–Sutcliffe efficiency.

3.2.3. Case Study: 2019 Validation Challenges

In 2019, model accuracy was again unsatisfactory. Although rainfall occurred between September 20–25, the observed inflow did not match the expected hydrograph. Two possible causes were identified: Rainfall was concentrated in the upper watershed, differing from the 2014 calibration year. Inflow data from the Royal Irrigation Department, derived using a water balance method, may have contained inaccuracies. The lower model performance during the 2019 and 2020 events can be attributed to several factors: spatial mismatch of rainfall, inflow estimation uncertainties, and limits

in calibration transfer. While ENSO phases may contribute, the limited number of events precludes strong inference.

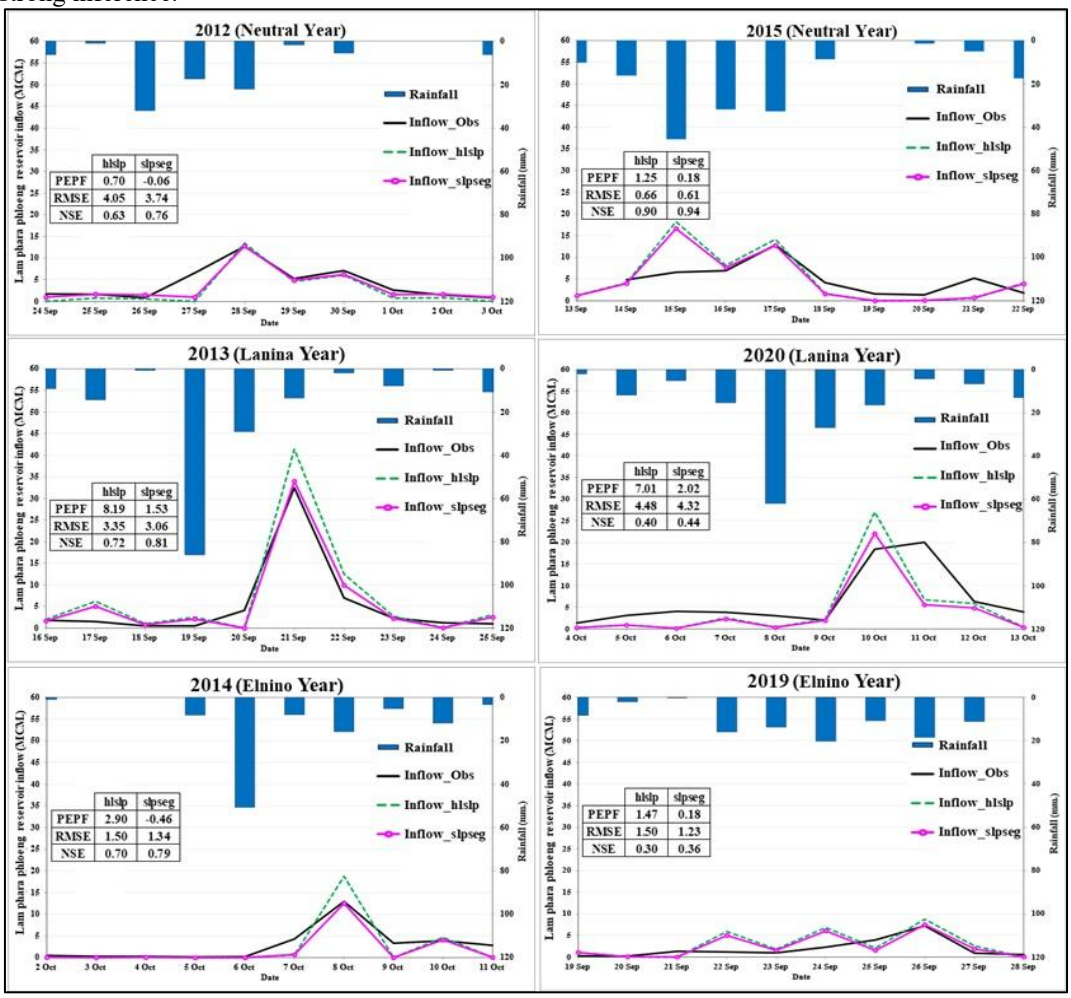

Fig. 9. Performance comparison of reservoir inflow prediction models using hillslope and slope segment methods.

3.2.4. Impact of Spatial Resolution on Model Performance

Subdividing the watershed into smaller slope segments increased spatial heterogeneity, allowing for more homogeneous units in terms of land use, soil group, and rainfall. This improved the representativeness of model parameters and enhanced prediction accuracy. For instance, within the same year, the slope segment model consistently produced lower PEPF values, indicating better alignment with observed peak inflows. This supports findings from Norris and Haan (1993), Kalin et al. (2003), Tripathi et al. (2006), who reported that finer spatial resolution improves peak inflow prediction—critical for reservoir management during the rainy season. Our slope segment method, relying on DEM-derived connectivity and standard CN values, is expected to transfer well to similar data contexts. Testing in contrasting physiography is suggested as future work.

3.2.5. Comparative Performance Metrics

RMSE: Lower in the slope segment model, indicating smaller deviations from observed inflows. NSE: Higher in the slope segment model, suggesting better overall prediction of total inflow volume. These results are consistent with studies by Bingner et al.,1997, Jha et al. (2004), and Rouhani et al. (2009), which found that models with larger sub-areas tend to overestimate total runoff volumes.

3.2.6. Summary on the comparison

The SCS CN method proved effective for inflow prediction in the Lam Phra Phloeng Reservoir. However, the slope segment-based model demonstrated superior accuracy compared to the hillslope-based model, particularly in representing spatial variability and predicting peak and total inflows. The event-based analysis further supports this conclusion, showing that improvements with slope segments were statistically significant across multiple rainfall events, not just isolated years. This strengthens confidence that the method enhances inflow prediction under a range of hydrological conditions.

4. CONCLUSIONS

The results demonstrate that slope segment discretization improved inflow prediction compared to hillslope units across all metrics. The main reason lies in the preservation of land use–soil heterogeneity at smaller scales. As shown in Table 3, slope segments retained distinct combinations (e.g., BA_crp) that were averaged out in hillslopes, leading to more representative CN values. This reduced aggregation error in estimating initial abstraction and effective rainfall, directly improving peak flow predictions. In addition, slope segments are delineated along local drainage links and contours, which enhances flow connectivity and the representation of hillslope hydrological processes. This explains why the slope segment model produced more realistic hydrograph shapes, with improved peak timing and magnitude. Similar findings have been reported in studies on the effect of grid size on runoff predictions (e.g., Hessel, 2005).

Although slope segments increased the number of modeling units, the computational burden remained acceptable within the semi-distributed framework. This suggests that slope segments may represent an optimal compromise scale: fine enough to capture local processes, but still efficient compared to fully distributed models. Years such as 2019 and 2020 showed weaker performance. While spatially uneven rainfall distribution likely played a role, other factors may also have contributed, including inflow data uncertainty and the transferability of calibrated CN parameters. We therefore refrain from attributing performance differences solely to ENSO phases, and suggest further testing with multi-year hydrographs. Overall, slope segments improve model fidelity by reducing spatial averaging errors, enhancing connectivity, and better representing heterogeneity in runoff generation. This supports our initial hypothesis and indicates strong potential for transferring the method to other watersheds with complex terrain and land-use mosaics.

REFERENCES

Amnatsan, S. (2021) Inflow forecasting of Bhavanisagar Reservoir using Artificial Neural Network (ANN). *Sustainable Practices and Innovations in Civil Engineering*, **79**, 119–131. https://doi.org/10.1007/978-981-15-5101-7_12

Arianti, I., Soemarno, Hasyim, A. W. & Sulistyono, R. (2018) Rainfall estimation by using Thiessen polygons, inverse distance weighted, spline, and kriging methods: A case study in Pontianak, West Kalimantan. *International Journal of Education and Research*, **6**, 301-310. https://ijern.com/journal/2018/November-2018/25.pdf

Beven, K. (1993) Prophecy, reality and uncertainty in distributed hydrological modelling. Advances in Water Resources, 16(1), 41–51. https://doi.org/10.1016/0309-1708(93)90028-E

Bingner, R., Garbrecht, J., Arnold, J. & Srinivasan, R. (1997) Effect of Watershed Subdivision on Simulation Runoff and Fine Sediment Yield. *Transactions of the ASAE*. **40**(5): 1329-1335. https://doi.org/10.13031/2013.21391

Chiamsathit, C. (2016). Optimisation of hedging-integrated rule curves for reservoir operation. PhD dissertation, Heriot-Watt University. https://www.ros.hw.ac.uk/bitstream/handle/10399/3168/ChiamsathitC_0616_egis.pdf?isAllowed=y&sequence=1

Crăciun, A.I., Haidu, I. & Bilaşco, Şt. (2007). The SCS-CN model assisted by G.I.S.– alternative estimation of the hydric runoff in real time. *Geographia Technica*, **2**(1), 1–7. https://technicalgeography.org/pdf/1_2007/gt_1_2007.pdf

Crăciun, A.I., Haidu, I., Magyari-Sáska, Zs. & Imbroane, A.I. (2009). Estimation of Runoff Coefficient According to Soil Moisture Using GIS Technique. *Geographia Technica*, **4**(2), 1–10. https://technicalgeography.org/pdf/2_2009/gt_2_2009.pdf

Ejaz, F., Wohling, T., Hoge, M. & Nowak, W. (2022) Lumped geohydrological modelling for long-term predictions of groundwater storage and depletion. *Journal of Hydrology*, 606. https://doi.org/10.1016/j.jhydrol.2021.127347

Fairfield, J. & Leymarie, P. (1991) Drainage networks from grid digital elevation models. *Water Resources Research*, 27, 709-717. https://doi.org/10.1029/90WR02658

Fan, Y., Clark, M., Lawrence, D. M., Swenson, S., Band, L. E., Brantley, S. L. & Yamazaki, D. (2019) Hillslope Hydrology in Global Change Research and Earth System Modeling. *Water Resources Research*, 1737-1772. https://doi.org/10.1029/2018WR023903

Flugel, W.A. (1995) Delineating hydrological response units by geographical information system analyses for regional hydrological modelling using PRMS/MMS in the drainage basin of the River Brol, Germany. *Hydrological Processes*, **9**, 423-436. https://doi.org/10.1002/hyp.3360090313

Fong, A. & Kawata, Y. (2019) Assessing the Influence of Cell Size on Flood Modelling by the PWRI-DH Model Using IFAS. *Journal of Disaster Research*, 14, 188-197.

Haidu, I. & Ivan, K. (2016). Urban runoff pathways and surface water volumes evolution. Case study: Bordeaux 1984–2014, France. (Évolution du ruissellement et du volume d'eau ruisselé en surface urbaine. Étude de cas : Bordeaux 1984-2014, France). *La Houille Blanche*, **5**, 51–56. https://doi.org/10.1051/lhb/2016050

Haidu, I., Batelaan, O., Crăciun, A.I. & Domnița, M. (2017). GIS module for the estimation of the hillslope torrential peak flow. *Environmental Engineering and Management Journal*, **16**(5), 1137–1144. https://eemj.eu/index.php/EEMJ/article/view/3269

Hessel, R., (2005), Effects of grid cell size and time step length on simulation results of the Limburg soil erosion model (LISEM), Journal Hydrological Processes. 19, 3037–3049. https://doi.org/10.1002/hyp.5815

Hutchinson, M.F. (1988) Calculation of Hydrologically Sound Digital Elevation Models. In *Third International Symposium on Spatial Data Handling*, August 17-19, 1988, Sydney, 117-133. https://www.researchgate.net/publication/242529374_Calculation_of_Hydrologically_Sound_Digital_Elevation_Models

Hutchinson, M.F. (1989) A new procedure for Gridding Elevation and Stream Line Data with Automatic Removal of Spurious Pits. *Journal of Hydrology*, **106**(3-4), 211-232. https://doi.org.10.1016/0022-1694(89)90073-5

Jha, P., Gassman, M. & Secchi, S. (2004) Effect of Watershed Subdivision on SWAT Flow, Sediment, and Nutrient Predictions. *Journal of the American Water Resources Association*, 811-825. https://doi.org/10.1111/j.1752-1688.2004.tb04460.x

Kalin, L. & Hantush, M.M. (2003) Assessment of Two Physically-Based Watershed Models Based on Their Performances of Simulating Water and Sediment Movement. In Proceedings, *First Interagency Conference on Research in the Watersheds*, Benson, AZ, October 27 - 30, 2003. USDA Agricultural Research Service, Washington, DC, 316-322. https://www.tucson.ars.ag.gov/icrw/Proceedings/Kalin.pdf

Kienzle, S. (2003) The Effect of DEM Raster Resolution on First Order, Second Order and Compound Terrain Derivatives. *Transactions in GIS*, 8, 83-111. https://doi.org/10.1111/j.1467-9671.2004.00169.x

Kocyigit, M.B., Akay, H. & Yanmaz, A.M. (2017) Effect of watershed partitioning on hydrologic parameters and estimation of hydrograph of an ungauged basin: a case study in Gokirmak and Kocanaz, Turkey. *Arab J Geosci* **10**, 331 (2017). https://doi.org/10.1007/s12517-017-3132-8

Kompor, W. (2021) Use of seasonal streamflow forecast to support reservoir operation for flood mitigation in the Chao Phraya River basin. PhD dissertation, Tokyo Institute of Technology.

Lapides, D., Sytsma, A., Neil, G., Djokic, D., Nichols, M. & Thompson, S. (2022) Arc Hydro Hillslope and Critical Duration: New tools for hillslope-scale runoff analysis. *Environmental Modelling and Software*, 153. https://doi.org/10.1016/j.envsoft.2022.105408

Lian, H., Yen, H. Huang, J.C., Feng, Q., Qin, L., Bashir, M.A., Wu, S., Zhu, X., Luo, J., Di,H., Lei, Q. & Liu, H. (2020) CN-China: Revised runoff curve number by using rainfall-runoff events data in China. *Water Research*, 177. https://doi.org/10.1016/j.watres.2020.115767

Moriasi, D.N., Arnold, J.G., Van Liew, M.W., Bingner, R.L., Harmel, R.D. & Veith, T.L. (2007) Model evaluation guidelines for systematic quantification of accuracy in watershed simulations, *Transactions of the ASABE*, 50(3), pp. 885–900. https://doi.org/10.13031/2013.23153

Nash, J.E. & Sutcliffe, J.V. (1970) River flow forecasting through conceptual models: Part I. A discussion of principles. *Journal of Hydrology*, 10, 282–290. https://doi.org/10.1016/0022-1694(70)90255-6

Ngamsanroaj, Y. Tamee, K. (2019) Improved Model using Estimate Error for Daily Reservoir Inflow Forecasting. https://doi.org/10.37936/ecti-cit.2019132.198508

ECTI Transactions on Computer and Information Technology, 13(2), 170-177.

Phomcha, P. (2021) Suitability of SWAT Model for Simulating of Monthly Streamflow in Lam Sonthi Watershed. *Journal of Industrial Technology*, 7(2), 49-56. https://ph01.tci-thaijo.org/index.php/jit_journal/article/view/3555

Reggiani, P., Sivapalan, M. & Majid Hassanizadeh, S. (1998) A unifying framework for watershed thermodynamics: balance equations for mass, momentum, energy and entropy, and the second law of thermodynamics. Advances in Water Resources, 22(4), 367–398. https://doi.org/10.1016/S0309-1708(98)00012-8

Rouhani, H., Willems, H. & Feyen, J. (2009) Effect of Watershed Delineation and Areal Rainfall Distribution on Runoff Prediction Using the SWAT Model. *Hydrology Research*, 40(6), 505-519. https://doi.org/10.2166/nh.2009.042

Searcy, J. K. & Hardison, C. H. (1960) Double Mass Curves. Manual of hydrology: Part 1. General Surface Water Techniques. US Geological Survey, Water-Supply Paper. https://www.scirp.org/reference/referencespapers?referenceid=396974

Sing, J., Knapp, H.V., Arnold, J. & Misganaw, D. (2004) Hydrologic Modeling of the Iroquois River Watershed Using HSPF and SWAT. Illionois State Water Survey. Champaign, IL, 8. https://www.isws.illinois.edu/pubdoc/cr/iswscr2004-08.pdf

Smith, M.B., Seo, D.J., Koren, V.I., Reed, S.M., Zhang, Z., Duan, Q., Moreda, F. & Cong, S. (2004) The distributed model intercomparison project (DMIP): motivation and experiment design. Journal of Hydrology, **298**(1-4), 4–26. https://doi.org/10.1016/j.jhydrol.2004.03.040

Soil Conservation Service. (1986) Urban Hydrology for Small Watersheds. Technical Release No.55. U.S. Department of Agriculture, Washington, D.C. https://www.hydrocad.net/tr-55.htm

Suiadee, W. & Tingsanchali, T. (2007) A combined simulation–genetic algorithm optimization model for optimal rule curves of a reservoir: a case study of the Nam Oon Irrigation Project, Thailand. *Hydrological Processes*, **21**(23), 3211–3225. https://doi.org/10.1002/hyp.6528

Tantasirin, C., Nagai, M., Tipdecho T. & Tripathi, N.K. (2016) Reducing hillslope size in digital elevation models at various scales and the effects on slope gradient estimation. *Geocarto International*, **31**(2), 140-157. https://doi.org/10.1080/10106049.2015.1004133

Tripathi, M., Rghuwanshi, N. & Rao, G. (2006) Effect of Watershed Subdivision on Simulation of Water Balance Components. *Hydrological Processes*, **20**(5), 1137-1156. https://doi.org/10.1002/hyp.5927

United States Department of Agriculture, Natural Resources Conservation Service. (2004) National Engineering Handbook, Part 630 Hydrology. https://directives.nrcs.usda.gov/sites/default/files2/1712930634/Part%20630%20-%20Hydrology.pdf

Vannametee, E., Karssenberg, D. & Bierkens, M.F.P. (2012) Towards closure relations in the Representative Elementary Watershed (REW) framework containing observable parameters: Relations for Hortonian overland flow. *Advances in Water Resources*, **43**, 52–66. https://doi.org/10.1016/j.advwatres.2012.03.029

Vannametee, E., Karssenberg, D., Hendriks, M.R. & Bierkens, M.F.P. (2013) Hortonian runoff closure relations for geomorphologic response units: evaluation against field data. *Hydrology and Earth System Sciences*, **17**(7), 2981–3004. https://doi.org/10.5194/hess-17-2981-2013

Wang, X. & Liu, J. (2006) An efficient method for identifying and filling surface depressions in digital elevation models for hydrologic analysis and modelling. International Journal of Geographical Information Science, 20(2), 193–213. https://doi.org/10.1080/13658810500433453

Wang, M., Shi, W., Zhao, Y., Yu, J., Chen, T., Bao, J., Song, W. & Chen, H. (2025) A modified curve number method for runoff prediction of different soil types in China. *Catena*, 254. https://doi.org/10.1016/j.catena.2025.108957

Wannasin, C., Brauer, C.C., Uijlenhoet, R., Verseveld, W.J. & Weerts, A.H. (2021) Daily flow simulation in Thailand Part I: Testing a distributed hydrological model with seamless parameter maps based on global data. *Journal of Hydrology*, **34**. https://doi.org/10.1016/j.ejrh.2021.100794

Zehe, E., Ehret, U., Pfister, L., Blume, T., Schroder, B., Westhoff, M. & Kleidon, A. (2014) HESS Opinions: From response units to functional units: a thermodynamic reinterpretation of the HRU concept to link spatial organization and functioning of intermediate scale catchments. *Hydrol Earth Syst Sci*, **18**(11), 4635–4655. https://doi.org/10.5194/hess-18-4635-2014

Zhang, H.L., Wang, Y.J., Wang, Y.Q., Li, D.X. & Wang X.K. (2013) The effect of watershed scale on HEC–HMS calibrated parameters: A case study in the Clear Creek watershed in Iowa, US. *Hydrol Earth Syst Sci*, **17**(7), 2735–2745. https://doi.org/10.5194/hess-17-2735-2013